Nuclear Instruments and Methods in Physics Research A 365 (1995) 49–53

NUCLEAR INSTRUMENTS & METHODS IN PHYSICS RESEARCH Section A

ELSEVIER

A cryogenic storage cell for polarized internal gas targets

L.H. Kramer [a,*], J.F. Kelsey [a], R.G. Milner [a], P. Winn [b], J. McGuire [b]

[a] *MIT-Bates Linear Accelerator Center and Laboratory for Nuclear Science, Massachusetts Institute of Technology, Cambridge, MA 02139, USA*

[b] *Applied Engineering Technologies, Ltd., 155B New Boston Road, Woburn, MA 01801, USA*

Received 26 April 1995

Abstract

A prototype cryogenically-cooled storage cell for the HERMES polarized ^{3}He internal target has been designed and constructed. The storage cell operates at 15 K with a 10 W applied heat load, while maintaining less than a 3 K differential over the 40 cm long cell. When operated at 15 K, the target thickness in the storage cell is a factor of 4.5 larger than for a room temperature cell. The cooling system used a continuous flow cryogenic helium gas loop. Complete details of the system are presented.

1. Introduction

Internal gas targets are being utilized in many of the next generation electron storage ring experiments because they realize the ideal interaction between beam and target. In these targets, a source of chemically and isotopically pure nuclei is directed into a windowless conductance limiter (the storage cell) through which the stored electron beam passes. In the storage cell the beam and target interact in the presence of no additional nuclei, hence the distinction "ideal interaction." When the injected gas is polarized the internal target provides an excellent platform for high precision spin measurements. The purity of the target implies that no dilution of the measured asymmetries arises from unpolarized target nuclei, and hence, no kinematic deconvolution is necessary to extract physics results. Additionally, the target polarization is rapidly reversible, which reduces systematic errors. Experiments planned at the HERA ring at DESY, the MIT-Bates South Hall Ring, and the NIKHEF AmPS. will utilize internal gas targets [1–3]. These experiments will exploit the low luminosity of the targets by using large acceptance detectors to simultaneously measure quantities over a broad kinematic range. The targets will also allow for detection of small-scattering angle and recoil particles as the storage cell designs incorporate thin-walled windowless structures.

The HERMES experiment will employ internal polarized targets to measure the spin-dependent structure functions of the neutron and proton by scattering 27 GeV longitudinally polarized electrons from polarized hydrogen, deuterium, and ^{3}He nuclei [1]. The internal targets for HERMES are based on an atomic beam source and a laser optically pumped ^{3}He target. The HERMES polarized ^{3}He target uses a laser-pumped metastability exchange source [4]. The stored beam lifetime limits the target thickness. To overcome this limitation the target is cryogenically cooled to 15 K, increasing the target thickness by a factor of 4.5 over a room temperature target without increasing gas load to the pumping system. The cooling is limited to 15 K by surface relaxation effects, which become important below $\sim$ 10 K. In this paper, we report on a prototype cryogenic internal storage cell for the HERMES ^{3}He target which will be installed in the HERA ring at DESY, Hamburg, Germany. Details of the system along with a series of cryogenic measurements are reported.

2. The storage cell design

In an internal gas target, the gas molecules are injected into a T-shaped storage cell. The gas is confined by the storage cell to the region close to the beam axis, resulting in an increase of the areal target density by two orders of magnitude over a free jet. For the HERMES detector, the storage cell design constraints include minimal material in the acceptance of the detector system, ultra-high vacuum compatibility, and minimal magnetic content in the materials used. The acceptance of the HERMES detector covers a rectangular region from 40 to 140 mrad in the vertical plane and $\pm$170 mrad in the horizontal plane over the entire target length. This far-forward looking geometry

* Corresponding author. Tel. +1 617 253 3761, e-mail kramer@mitlns.mit.edu.

0168-9002/95/$09.50
SSDI 0168-9002(95)00498-X

requires the use of minimal materials in the acceptance, since particles may shower in the material, generating background in the detector system. Ultra-high vacuum compatibility is necessary for interfacing with the ring and maintaining long beam lifetimes. Magnetic material is minimized because holding field inhomogeneities limit target polarization.

To further increase the target density the storage cell is cooled to 15 K, increasing the target density by a factor of 4.5. Our cooling system is designed to operate at 15 K and accommodate up to 10 W of heating along the storage cell, with no more than a 3 K temperature differential over the entire 40 cm long cell. The heating of the storage cell is generated by wakefields created by the time structure of the stored beam. This heating is minimized by having smooth transitions between beamline components. Calculations [1] show that the heating is expected to be on the order of several W over the target cell, therefore a conservative design goal of 10 W is used. The minimum temperature for the cooling cell is determined by surface relaxation effects. We now briefly examine this subject.

At low temperatures the relaxation time of polarized ^{3}He atoms on copper has been measured over the temperature range 13–40 K [5]. Using these data we estimate the depolarization probability/wall collision to be 5×10^{-6} at 13.5 K on copper. A ^{3}He atom typically has $\sim 10^3$ wall collisions as it traverses the target. Assuming that depolarization probability per wall collision for ^{3}He on aluminum is similar to that on copper we estimate that the lowest operating temperature for negligible wall depolarization is $\sim$ 10–15 K.

A thin-walled elliptical storage cell has been fabricated to meet these design specifications. The cell was a 29.0 mm $\times$ 9.8 mm elliptical tube, with a feed tube intersecting at the center, where the size corresponds to a $\pm 20\sigma$ clearance for beam during injection. It was constructed from two sheets of ultra-pure (99.9999%), thin (127.0 μm) aluminum which were formed into half ellipses with half tubes at the center. The halves were spot welded together, forming the desired shape (see Fig. 1) where the flat sections support the target and allow for cooling. The target was supported at its edges by long rails which also provided the cooling. Ultra-pure aluminum was used due to its excellent thermal conduction properties at cryogenic

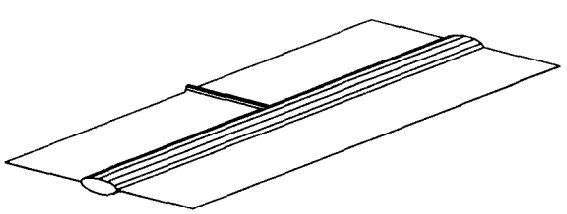

Fig. 1. Internal target storage cell. The cell is formed from 2 sheets of ultra-pure (99.9999%), thin (127.0 μm) aluminum, spot welded together.

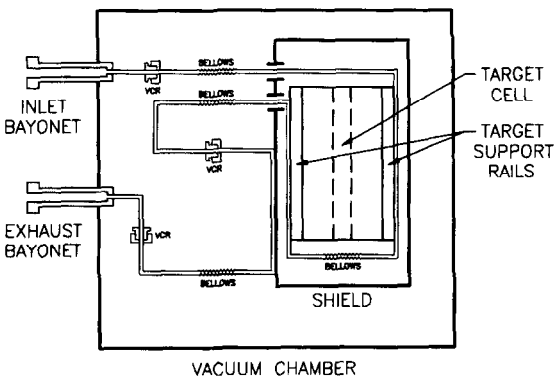

Fig. 2. The cryogenic internal target storage cell cooling loop.

temperatures and low atomic number which minimizes showering. In the region of interest (around 15 K), the ultra-pure aluminum is over thirty times more conductive than commercial pure (99%) aluminum [6]. In the next section, we describe the cryogenic cooling system.

3. The cryogenic cooling system design

The storage cell cooling system was based on a cryogenic helium gas continuous flow loop. Cryogenic helium gas entered the system through a bayonet fitting and was directed to the storage cell support rails, which allowed for cooling of the storage cell. The exhaust from the storage cell rails was connected to the radiation shield plate which minimized radiant heating. After leaving the radiation shield plate, the helium gas left the chamber through a second bayonet fitting and was vented to atmosphere. The cooling loop is shown in Fig. 2. We now describe the storage cell support system and cooling loop.

The storage cell support system is shown in Fig. 3. The storage cell was supported with two sets of aluminum rails, clamping the cell along its the edges. A set of eight

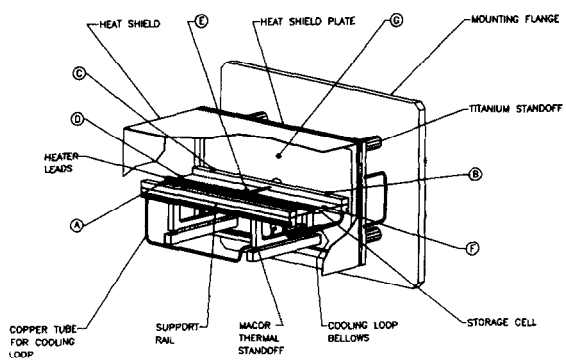

Fig. 3. Support system for the cryogenic internal target storage cell. Also shown are the locations of the heater and silicon diode temperature sensors used in testing.

fasteners were used for each rail to ensure good thermal contact between the rails and target. The rails were positioned outside the limits of the detector acceptance. These rails were supported by two U-shaped aluminum brackets, which were attached to a set of cantilevered aluminum beams. The brackets were thermally isolated from the beams via a set of nickel-flashed ceramic washers. The beams were attached to an aluminum radiation shield support plate. The shield plate was mounted to the vacuum flange plate with a set of four thin-walled titanium posts. The shield plate also supported the radiation shield, which encapsulated the storage cell. The storage cell alignment was adjusted through use of several slotted holes on the support beams and shield plate. Titanium fasteners were used in the support system because of their non-magnetic properties.

The cooling loop consisted of 3/16 in. oxygen free, high conductivity (OFHC) copper tubing segments which were soldered onto the various components and then connected to form a loop. The cooling loop began at the entrance bayonet fitting where 3/16 in. OFHC copper tubing was soldered to the fitting. The tubing passed through the radiation shield plate and the bottom two clamping rails, where it was silver soldered to U-shaped channels in the rails. The rails were nickel flashed to allow for soldering. The tubing extended down one rail and returned along the opposite rail, with a bellows joint in the section between the rails. The loop passed through the shield plate and was silver soldered to U-shaped channels in the plate which was also nickel flashed. This allowed the cooling exhaust from the cell support to cool the radiation shield, eliminating the necessity for a separate radiation shield cooling loop. The radiation shield had view factor control sleeves on all penetrations to minimize thermal radiation onto the target, and three 3 in. diameter view shielded vent holes to allow for efficient pumpout of the storage cell area. The loop ended at the exhaust bayonet. Also included in the loop were several bellows to allow for thermal expansion and several stainless steel $\frac{1}{4}$ in. Cajon VCR fittings to allow for disassembly. All joints were soldered with cadmium-free silver solder to ensure ultra-high vacuum compatibility. The complete system was mounted on one flange to allow for easy assembly and disassembly on the vacuum chamber.

4. Cryogenic testing

A series of tests was carried out to determine the performance characteristics of the system. A heater and a set of sensors were attached to the system for these tests. To simulate heating, a nichrome wire was attached to the center of the storage cell and a current was passed through it. The current was varied to simulate various heat loads from 0 to 10 W. A set of seven silicon diode temperature sensors (Lakeshore P/N DT-471-CU) were attached to the storage cell and support structure to monitor the temperature during testing. Three sensors were mounted near the center of the storage cell (on the flat region next to the elliptical tube), one at each end (sensors D and F) and one in the center (sensor E). Three sensors were mounted on the clamping bars, one at the coolant inlet of the first rail (sensor A), another at the second rail coolant inlet (sensor B), and one at the coolant outlet of the second rail (sensor C). The remaining sensor was placed on the radiation shield plate (sensor G). Sensor and heater locations are shown in Fig. 3. Helium use was monitored with a mass flowmeter placed in the exhaust line.

Initial cooldown was accomplished by flowing liquid nitrogen through the system. This pre-cooling stage was complete when liquid nitrogen flowed from the outlet line and typically took from 35 to 45 minutes to reach ~ 90 K when starting at room temperature. After the liquid nitrogen cooldown, liquid helium was introduced into the system from a dewar overpressured by $\frac{1}{3}$ atm. The liquid helium was used to cool the system to ~ 20 K. At this point, the transfer tube was raised above the liquid helium level in the dewar, to allow cooling by gaseous helium. Use of the gaseous helium was necessary because preliminary tests showed that the system exhibited instabilites under liquid helium cooling, which is a common problem with cryogenic systems [7]. The instabilities arise from the liquid helium boiling, creating shock waves in the liquid medium which feedback and oscillate. While these instabilities can be removed by careful design considerations, we found that it was much simpler to use gaseous helium. The gaseous helium provided a stable system, where the cooling power was only slightly diminished due to the low latent heat of helium. The gaseous helium can be flow regulated by either pumping on the exhaust of the system or by pressurizing the storage dewar. In our tests, we chose the simpler method of pressurizing the storage dewar by installing a resistive heater in the dewar and applying current to regulate flow. This resulted in a very stable and reliable regulated system. For the HERMES experiment, the flow will be regulated by pumping on the exhaust of the cooling system. This will be necessary because of fluctuations in the helium gas return system pressure, which can adversely affect the cooling system. Pumping effectively decouples the storage cell cooling system from the helium gas return system.

The tests were conducted by flowing the cryogenic helium gas through the system and varying both the helium flow rate and heat applied to the storage cell. Results for the complete set of temperature sensors are given in Table 1. The sensor locations are illustrated in Fig. 3. Temperatures along the center of the cell are given by sensors D, E, and F. Sensor D consistently reads slightly higher than sensors E and F because the nichrome heater wire extended beyond the cell near this sensor and hence produced a higher heat load in that region of the target. A similar effect is seen for sensors A and C, although the

effect on sensor A is not as dramatic as it is located near the helium input. Results for the central (E) sensor as a function of heat applied and flow rate are shown in Fig. 4. We first note that the system exceeds the design specification. Flowing 193 standard liters per minute (SLPM) of helium gas (corresponding to 16.5 liquid-liters of helium per hour) with a 10 W heat load produces a central temperature of 11.3 K with a temperature difference of only 0.1 K between sensors E and F. Under a more reasonable heat load estimate of 2 W, the system requires only 80 SLPM (6.9 liq.-liters/hour) helium to maintain 14.6 K. We also see that the system exhibits essentially linear behavior in heat load and flow rate.

Table 1
Temperatures for the seven sensors as a function of helium gas flow and heat applied to the storage cell. Sensor locations are described in the text and shown in Fig. 3. Helium gas flow rates are given in standard liters per minute

Helium flow [SLPM]	Heat applied [W]	Sensor temperature [K]						
		A	B	C	D	E	F	G
65	0.0	16.0	16.2	18.1	17.8	16.1	16.3	41.5
65	1.0	16.7	17.1	18.8	18.6	16.9	17.0	41.4
65	2.0	17.6	17.8	19.4	19.2	17.8	17.9	41.5
65	5.0	19.9	20.0	22.9	22.6	20.4	20.4	42.0
65	10.0	27.7	27.8	28.9	29.0	28.3	28.2	43.3
80	0.0	12.4	11.0	14.9	14.5	12.5	12.7	30.4
80	1.0	13.4	13.8	15.9	15.5	13.5	13.7	30.5
80	2.0	14.4	14.6	16.7	16.4	14.6	14.7	30.6
80	5.0	16.8	16.9	18.8	18.5	17.1	17.1	30.8
80	10.0	22.2	22.7	26.7	26.5	23.4	23.1	31.4
102	0.0	9.7	9.0	12.1	11.7	8.8	9.9	29.3
102	1.0	10.4	9.5	13.1	12.7	10.1	10.8	29.4
102	2.0	11.3	9.9	14.0	13.6	9.8	11.7	29.6
102	5.0	13.6	13.8	16.2	15.8	13.8	13.9	30.0
102	10.0	16.9	16.9	19.1	18.9	17.2	17.1	30.4
112	0.0	9.4	9.6	11.6	11.1	9.5	9.6	30.4
112	1.0	9.8	10.1	12.4	11.9	9.9	10.1	30.3
112	2.0	10.5	10.9	13.2	12.8	10.7	10.9	30.3
112	5.0	12.7	12.9	15.3	14.9	12.9	13.0	30.3
112	10.0	15.6	15.5	17.9	17.6	15.9	15.9	30.4
132	0.0	8.1	7.6	9.8	9.5	7.5	8.5	25.0
132	1.0	8.8	8.0	10.6	10.1	8.9	9.0	25.2
132	2.0	9.2	8.5	11.5	11.0	9.4	9.5	25.6
132	5.0	11.0	9.7	13.8	13.4	9.7	11.4	27.1
132	10.0	14.3	14.3	16.9	16.6	14.6	14.5	28.5
158	0.0	7.5	6.9	9.0	8.5	6.7	7.7	20.0
158	1.0	7.9	7.6	9.5	9.1	8.0	7.3	20.2
158	2.0	7.5	7.7	10.0	9.7	8.5	7.7	20.6
158	5.0	9.7	8.8	12.4	12.0	9.8	9.9	21.9
158	10.0	12.8	12.6	15.7	15.3	13.1	13.1	24.5
193	0.0	6.8	6.3	8.3	7.7	6.0	6.2	18.2
193	1.0	7.2	6.6	8.7	8.2	7.3	6.6	18.2
193	2.0	7.6	6.9	9.2	8.7	7.7	6.9	18.3
193	5.0	8.7	7.9	10.7	10.2	8.9	7.9	18.7
193	10.0	11.0	9.5	14.0	13.6	11.3	11.2	19.6

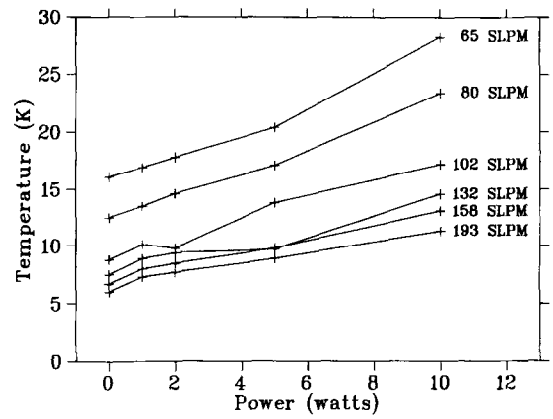

Fig. 4. Temperature as a function of heat applied to the storage cell, for several cryogenic helium gas flow rates. Temperature is given for the central (E) sensor and the flow rates are in standard liters per minute of helium.

5. Conclusion

We have designed and constructed a prototype cryogenic internal storage cell for the HERMES experiment at DESY. The system exceeds the design goals of maintaining 10 K under a 10 W heat load with less then a 3 K temperature differential over the storage cell. For a 10 W heat load the target requires 132 SLPM (11.3 liq.-liters/hour) helium to maintain 14.6 K. At the expected heating level of 1–2 W the target requires 5.5–7.0 liquid-liters of helium per hour to maintain 15 K. The system can easily be adapted for other target systems, including those which call for higher heat loads and lower temperatures. Current plans include using modified versions of the system for the internal polarized ^{3}He target for the Bates Large Acceptance Spectrometer Toroid detector at the MIT-Bates South Hall Ring [8] and for an external polarized ^{3}He target currently proposed for the CLAS detector at CEBAF [9].

Acknowledgements

The authors would like to thank G. Sechan (MIT) for constructing the storage cells used for testing. This work supported by the MIT Sloan Fund and by the United States Department of Energy under cooperative agreement No. DE-FC02-94ER40818.

References

[1] HERMES proposal to DESY, DESY-PRC-90-01, unpublished 1990.
[2] J.F.J. van den Brand, R.G. Milner et al., Bates proposal 89-12, December 1989.
[3] J.F.J. van den Brand, C. de Jager et al., NIKHEF proposal 91-12, 1991.
[4] K. Lee, J.O. Hansen, J.F.J. van den Brand and R.G. Milner, Nucl. Instr. and Meth. A 333 (1993) 294.
[5] C.E. Jones et al., Phys. Rev. C 47 (1993) 110.
[6] J.E. Jensen et al., Brookhaven National Laboratory Selected Cryogenic Data Notebook, Brookhaven National Laboratory Report #10200-R, Vol 1, 1980.
[7] B.A. Hands, Cryogenic Engineering (Academic Press, London, 1986).
[8] Bates Large Acceptance Spectrometer Toroid (BLAST) proposal, September 1991.
[9] CEBAF proposal 89-020, spokesman R.D. McKeown.